# Enhancing photovoltaic system maximum power point tracking with fuzzy logic-based perturb and observe method

**Muhammad Ihsan Aziz Jafar[1], Muhammad Iqbal Zakaria[1], Nofri Yenita Dahlan[2], Muhammad Nizam Kamarudin[3], Nabil El Fezazi[4,5]**
[1]School of Electrical Engineering, College of Engineering, Universiti Teknologi MARA, Shah Alam, Malaysia
[2]Solar Research Institute, Universiti Teknologi MARA, Shah Alam, Malaysia
[3]Faculty of Electrical Technology and Engineering, Universiti Teknikal Malaysia Melaka, Melaka, Malaysia
[4]Higher School of Technology, Ibn Zohr University, Dakhla, Morocco
[5]Faculty of Sciences Dhar El Mehraz, Sidi Mohammed Ben Abdellah University, Fez, Morocco

**Article Info**

***Article history:***

Received Jun 28, 2023
Revised Jan 10, 2024
Accepted Jan 12, 2024

***Keywords:***

DC-DC converter
Fuzzy logic controller
MATLAB/Simulink
Maximum power point tracking
Perturb and observe
Photovoltaic system

**ABSTRACT**

Photovoltaic systems have emerged as a promising energy resource that caters to the future needs of society, owing to their renewable, inexhaustible, and cost-free nature. The power output of these systems relies on solar cell radiation and temperature. In order to mitigate the dependence on atmospheric conditions and enhance power tracking, a conventional approach has been improved by integrating various methods. To optimize the generation of electricity from solar systems, the maximum power point tracking (MPPT) technique is employed. To overcome limitations such as steady-state voltage oscillations and improve transient response, two traditional MPPT methods, namely fuzzy logic controller (FLC) and perturb and observe (P&O), have been modified. This research paper aims to simulate and validate the step size of the proposed modified P&O and FLC techniques within the MPPT algorithm using MATLAB/Simulink for efficient power tracking in photovoltaic systems.



***Corresponding Author:***

Muhammad Iqbal bin Zakaria
School of Electrical Engineering, College of Engineering, Universiti Teknologi MARA
Shah Alam, Malaysia
Email: iqbal.z@uitm.edu.my

## 1. INTRODUCTION

The growing need for energy and the possibility of a decrease in the supply of conventional fuels, as demonstrated by the problems with natural gas, coal, and petroleum, have spurred research and development of renewable, cleaner, and less environmentally harmful alternative energy sources [1]–[3]. Additionally, among the alternative energy sources, the currently thought to be a more practical natural energy source is the generation of electrical energy from photovoltaic (PV) cells because it is plentiful, available for free, clean and is dispersed throughout the earth. It also plays a crucial role in every other method of generating energy on earth. Therefore, harnessing solar energy through photovoltaic cells has gained significant attention in the search for sustainable energy solutions. Moreover, despite the phenomena of sunlight absorption and reflection by the surrounding environment, the amount of solar energy that occurs on earth's surface is thought to be 10,000 times greater than global energy consumption [4].

Evaluation of photovoltaic source due to its nonlinear output features which alternate with atmospheric solar irradiation and temperature are another crucial component of using a photovoltaic source. When the PV array experiences non-uniform insolation, like in partially shadowed conditions, the characteristics grow more complex and result in several peaks [5]. The efficiency may be reduced due to existence of numerous peaks. Therefore, various methods have been established to monitor the maximum power point, including the perturb and observe (P&O) algorithm and fuzzy logic controller (FLC), which are commonly used in PV systems.

P&O algorithm able to be presented by processing actual values of photovoltaic current and voltage, regardless of atmospheric circumstances, type of photovoltaic panel or aging to track the maximum power point continuously. Due to its ease implementation and simplicity, it has been a common method used in the photovoltaic system. The process entails varying the PV array's voltage or current, either up or down, and comparing the resultant PV output power to the power from the preceding perturbation cycle [6]. If the operating voltage changes and the power increases, the control system will tilt the solar array's operating point in that direction; if not, it will move it in a different direction. The following perturbation cycle of the algorithm is conducted in the same way. The benefits of the P&O method include its simplicity, ease of implementation and control, low cost, and high output power [7], [8].

Since the FLC is robust, simple to construct, and able to handle nonlinearity and defective inputs without requiring an exact mathematical model, it has also been frequently utilized by PV systems to monitor the maximum power point [9], [10]. The FLC technique consists of three stages: fuzzification, aggregation and defuzzification. A membership function created during fuzzification stage to convert the numerical input variables. The input and output system are linguistically related. Rules are the relationships and a fuzzy set is the result of each rule. Therefore, numerous rules are applied to improve conversion efficiency. A separate output of fuzzy set is created by aggregating the fuzzy sets produced by each rule, which is called as aggregation process. The defuzzification method subsequently sharpens the output from the fuzzy set [11]–[13].

Driven by the literature survey mentioned earlier, in this paper, a modified method combining both the P&O algorithm and FLC has been developed. Due to limitations in the traditional perturb and observe approach, such as delayed convergence or ascent to the maximum power point, oscillation of photovoltaic power around the maximum power point under steady state that results in power loss, and rapid changes in maximum power point position due to fluctuating atmospheric conditions, a modified fuzzy logic controller based perturb and observe for maximum power point tracking has been established based variable step size. The layout of this paper is as follows: the paper consists of 5 parts, following with introduction, section 2 presents PV system description which consists of PV system, PV panel model and power converter. Besides, section 3 presents the fuzzy logic-based perturb and observes MPPT, while section 4, it consists of the discussion of the simulation result and findings which are obtained from MATLAB/Simulink. Lastly, section 5 presents the conclusion.

## 2. DESCRIPTION OF THE PHOTOVOLTAIC SYSTEM

### 2.1. Photovoltaic system

The photovoltaic system combined with a maximum power point tracking (MPPT) controller is displayed in Figure 1. When designing a photovoltaic system, two key aspects need to be considered: the modelling of the MPPT boost direct current to direct current (DC-DC) converter and the modelling of the photovoltaic array. The objective is to optimize power transmission by adjusting the load impedance to coincide with the peak power point [14].

### 2.2. PV panel model

Electrical energy can be generated through the conversion of solar energy, facilitated by solar photovoltaic technologies. These devices use solar cells to directly convert exposure to sunlight into DC electrical energy. The circuit architecture of a photovoltaic panel, which consists of resistors, diodes, and a current source, is shown in Figure 2. Photovoltaic cells employ a semiconductor structure, typically a p-n junction, to harness the energy from photons in sunlight. When exposed to solar radiation, the cells absorb photons, causing the mobilization of electrons and the subsequent generation of electricity. As a result, when a load is connected to a photovoltaic cell throughout the period of irradiance, electric charges flow as direct current. To achieve the desired voltage and current levels, the cells can be linked in either shunt or series configuration. Connecting the cells in series allows for higher output voltage, while connecting them in parallel enables higher output current.

The photovoltaic array's circuit structure is shown in Figure 2, allowing it possible to calculate $I_{pv}$, which stands for the array's output current. The equation (1) provides the derivation of $I_{ph}$, which represents the photogenerated current and is expressed as (1):

$$I_{ph} = \left(I_{sc} + k_i(T_c - T_{stc})\right)\left(\frac{G}{G_{stc}}\right) \tag{1}$$

where $T_c$ is the absolute operating temperature, $T_{stc}$ is the temperature at standard test condition (STC) which is 25 °C, $G$ is the irradiance, and $G_{stc}$ is the irradiance at STC which is 1,000 W/m². $I_{sc}$ is the short circuit current of the photovoltaic system. $k_i$ is the short circuit current coefficient. However, in indoor situations, the $I_{ph} \approx 0$, where the solar array's I-V characteristics are described using (2), (3), and (4):

$$I_{pv} = I_{cs} - I_o\left(e^{\frac{V_{pv}-I_{pv}R_s}{N_sV_t}} - 1\right) - I_{sh} \tag{2}$$

$$V_{pv} = (I_{cs} - I_{pv})R_s + nV_t ln\frac{(I_{cs}-I_{pv})-I_{sh}+I_o}{I_o} \tag{3}$$

$$I_{sh} = \frac{V_{pv}-(I_{cs}-I_{pv})R_s}{R_{sh}} \tag{4}$$

The equation $V_t = kT_c/q$ gives the junction thermal voltage, where $k$ is the Boltzmann's constant of $1.381 \times 10^{-23}\,J/K$ and $q$ is the elementary charge of $1.602 \times 10^{-19}\,C$. The dark saturation current is represented by $I_o$, the output current by $I_{cs}$, the panel series resistance by $R_s$, the panel shunt resistance by $R_{sh}$ and the number of cells connected in series by $N_s$. Table 1 presents the solar array's properties under STC.

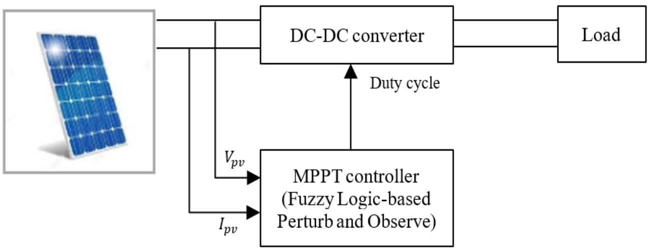


Figure 1. Photovoltaic system

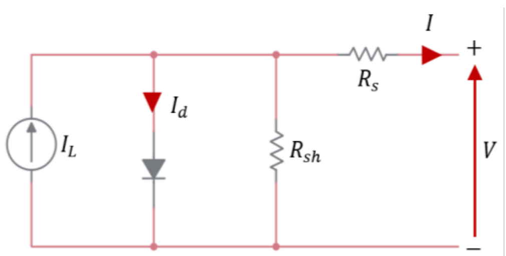


Figure 2. PV array modelling circuit

Table 1. Solar panel 1Soltech 1STH-250-WH specifications at STC

| Electrical characteristics | Parameters |
|---|---|
| Rated maximum power ($P_{max}$) | 250.205 W |
| Open-circuit voltage ($V_{oc}$) | 37.3 V |
| Short-circuit current ($I_{sc}$) | 8.66 A |
| Voltage at maximum power point ($V_{mpp}$) | 30.7 V |
| Current at maximum power point ($I_{mpp}$) | 8.15 A |
| Voltage temperature coefficient | -0.36901%/°C |
| Current temperature coefficient | 0.086998 |

### 2.3. DC-DC power converter

A circuit in the electrical system called a power converter takes a DC input and outputs a DC output with a distinct voltage. High frequency switching operations involving inductive and capacitive filter components are used to accomplish this transition. A power converter's function is to convert electric energy from one form to an optimized form that suits the specific load requirements. In the context of photovoltaic systems, one commonly used type of power converter is the DC-DC boost converter [15]. The fundamental arrangement of a DC-DC boost converter is depicted in Figure 3. It comprises two semiconductor devices, such as a transistor and a diode/IGBT, as well as an inductor, input and output capacitors, and a DC load connection. The boost converter operates by increasing the input DC voltage, given that the output voltage is greater than the source voltage, the converter is a step-up [16].

The DC-DC boost converter expression can be obtained as follows, where the duty rate of the switch and the voltage at the input determine the increase in the level of the output voltage.

$$V_o = V_i(1 - D) \tag{5}$$

When the condition of the IGBT/diode is turn on and $D$ in reverse biased in (6), (7) and (8), the output voltage determined from the equation's duty cycle and derivation input voltage.

$$\frac{di_L}{dt} = \frac{V_{pv}}{L} \quad (6)$$

$$\frac{dV_O}{dt} = -\frac{V_O}{RC_2} \quad (7)$$

$$I_{pv} = i_L + C_i \frac{dV_{pv}}{dt} \quad (8)$$

The equation (9) derived by correlate the relationship between the changing of inductor current with time and photovoltaic voltage with inductor when the condition of IGBT/diode turned off and $D$ is forward biased.

$$\frac{di_L}{dt} = \frac{V_{pv}}{L} - \frac{V_O}{L} \quad (9)$$

$$\frac{dV_O}{dt} = \frac{i_L}{C_2} - \frac{V_O}{RC_2} \quad (10)$$

The power converter regulates the movement of energy from the source of input to the load by changing the duty cycle $D$. In (12) show the simplified version of (11) where voltage of photovoltaic cell excluded.

$$V_{pv}t_{on} = (V_{out} - V_{pv}) \times t_{off} \quad (11)$$

$$V_{out} = \frac{t_{on}+t_{off}}{t_{off}} V_{pv} \quad (12)$$

$$T = t_{on} + t_{off} \quad (13)$$

The general equation of period stated in (13) where the turn-on time sum with turn-off time. Then, the (14) represents the difference of turn on-time and total time called as duty cycle, $a$

$$a = \frac{t_{on}}{T} \quad (14)$$

Then, from (12), the voltage produced can be derived as (15) where the duty cycle and solar cell input voltage are used to establish the output voltage.

$$V_{out} = \frac{1}{1-a} \quad (15)$$

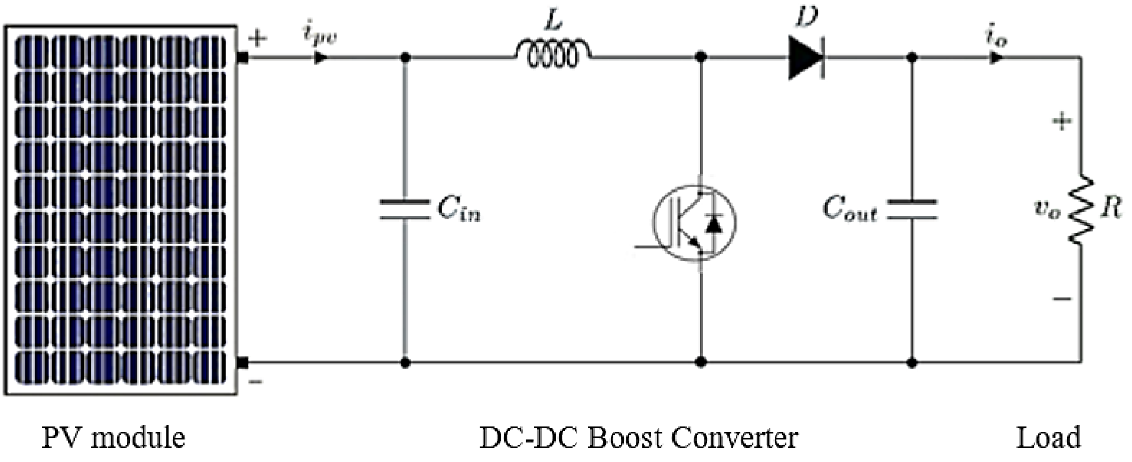


Figure 3. DC-DC boost converter

## 3. ALGORITHM OF VARIABLE STEP SIZE P&O BY UTILIZING FLC

### 3.1. Perturb and observe description

P&O approaches are commonly implemented to extract the maximum power point in a photovoltaic system due to its simplicity and minimal parameter requirements. The voltage of the array is periodically perturbed by either increasing or decreasing it, and the P&O algorithm contrasts the power from the prior perturbation cycle with the present solar output power [17]. The perturbation keeps going in the identical manner as the power increases; otherwise, it changes direction. As a result, each maximum power point tracking cycle induces a change in the terminal voltage of the array. In situations where atmospheric conditions exhibit continuous or gradual changes, the P&O algorithm will subsequently adapt, possibly resulting in the loss of photovoltaic power [18].

Taking into consideration the step size of voltage perturbation in Figure 4(a) as well as the I-V and P-V characteristic curves in Figure 4(b). Figures 4(a)-(b) show how to perturb and observe maximum power point tracking. It firmly shows that the output current and voltage of a solar photovoltaic system accurately characterize its electrical behavior under changing solar irradiation. When the solar source's terminal voltage is successfully managed to retain a level that maximizes the product of photovoltaic voltage and current, the maximum power point is reached. The knee point of the typical I-V curve for photovoltaic diodes is depicted in Figure 4(a)-(b), along with the limitations for open circuit voltage ($V_{oc}$) and short circuit current ($I_{sc}$) presented [19].

Analyzing the solar arrays voltage and output derivatives, which establishes an alteration in the operating point, is the fundamental idea underpinning P&O techniques for MPPT. This method involves periodically adjusting the photovoltaic array voltage by either increasing or decreasing it. The operating point will be to the left of the maximum power point (MPP) if an increase in the operating voltage causes an increase in output power. This means that additional voltage perturbations will be required to reach the MPP on the right. Conversely, in the situation where a spike in voltage causes a drop in power, the location of the center of operations will be to the right of the MPP, necessitating more perturbations to shift leftward and near the MPP [20], [21].

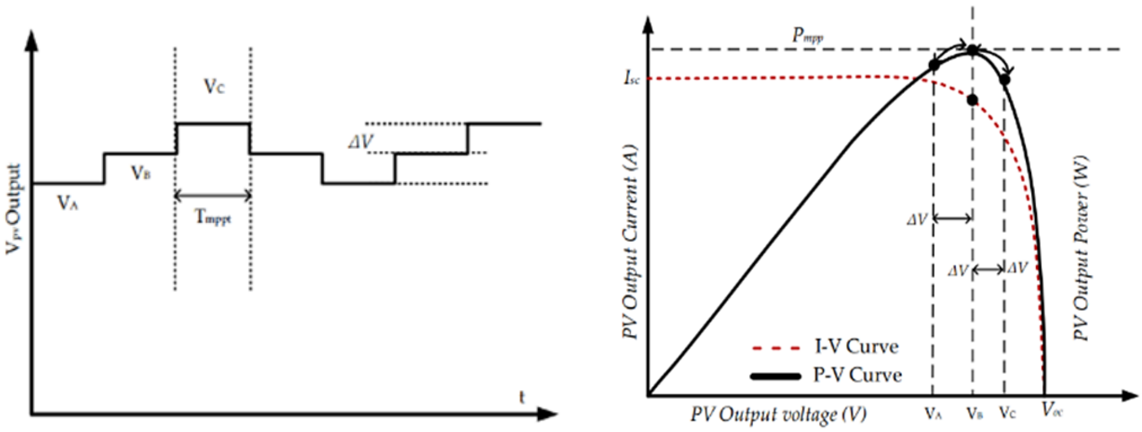


(a) (b)

Figure 4. P&O MPPT operation: (a) perturbation step ΔV and (b) I-V and P-V characteristics curve

### 3.2. Description of fuzzy logic controller

A notable control strategy based on artificial intelligence for tracking maximum power point is the FLC. Fuzzy logic, often known as fuzzy set theory, offers a new method for measuring peak power points. The translation of input variables, which include the first perturbation step size and the immediate observed slope of solar power, through linguistic values by fuzzification is illustrated in Figure 5 by the fuzzy logic controller's block design. This process involves the use of linguistic variables and fuzzy sets, which represent smooth changes in membership rather than abrupt transitions, forming the basis for fuzzy logic controllers [22]. The inference engine in the controller assesses the fuzzy rules and linguistic variable definitions to make decisions and determine the appropriate fuzzy control action. To obtain a non-fuzzy (crisp) control action that closely resembles the fuzzy one, a defuzzification technique is applied since a fuzzy controller produces a fuzzy set as its output. The final step involves obtaining the crisp value for the variable step size, which serves as the output of the controller.

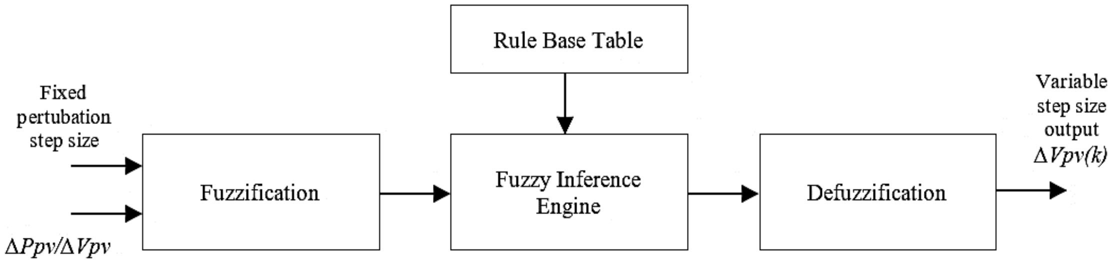


Figure 5. Block schematic of a fuzzy logic controller

An analytical method called fuzzy logic control makes it possible to include human reasoning and expertise into the development of nonlinear controllers [23]. Typically, fuzzy controller rules are expressed using linguistic terms. Commonly, two distinct kinds of fuzzy inference systems are employed: Sugeno and Mamdani. The Mamdani inference system synthesizes a collection of linguistic control rules defined by expert human operators, with each rule producing a fuzzy set as its output. This technique works especially well in expert applications for systems where the rules are derived from human skill and are easy to comprehend, like medical diagnostics [24]. Conversely, the Takagi-Sugeno-Kang inference system, also called the Sugeno inference system, employs single output membership functions, which may be unchanging factor or linear functions of the input values. Unlike the Mamdani system, which computes the centroid of a two-dimensional area, a weighted average or sum of a limited amount of data points is used in a Sugeno system, making it more computationally efficient [25].

Table 2 shows the fuzzy rule base table for maximum power point tracking. There are about 25 rules developed in the fuzzy logic toolbox to prescribe conclusion of the instantaneous voltage of the variable step size. The inputs indicate the step size perturbation and P-V curve slope while one output indicates variable step size.

Table 2. MPPT fuzzy rule base table

| $\boldsymbol{\Delta e = S(k)}$ <br> $\boldsymbol{E = Voltage\ Step}$ | PVS | PS | PM | PH | PVH |
|---|---|---|---|---|---|
| PVS | PVH | PVS | PVS | PS | PS |
| PS | PVH | PVS | PVS | PS | PS |
| PM | PS | PS | PS | PVH | PVH |
| PH | PS | PS | PVH | PVH | PVH |
| PVH | PVS | PVS | PVH | PVH | PVH |

where PH is for positive high, PS is for positive small, PVS is for positive very small PM is for positive medium, and PVH is for positive very high.

Figure 6 illustrates the flowchart of the fuzzy logic controller-based perturb and observe MPPT algorithm. This algorithm evaluates power variations and adjusts the operational voltage of a photovoltaic system by modifying the effective of the boost converter's input resistance through altering the switching device's duty cycle. The system initiates by measuring two parameters: voltage and current from the photovoltaic system. The flowchart provides a detailed explanation of the process.

In the beginning the fuzzy logic controller and the P&O technique are the two different paths that result from the voltage and current measurements. Various calculations are performed based on the measurements to determine the actual power (Ppv (k)), the changes in power (Δ Ppv (k)), and the changes in voltage (Δ Vpv (k)). In these computations, the immediate voltage and current measurements are incorporated with corresponding prior values. The two inputs that the fuzzy logic controller obtains are the perturbation step size and the slope, which is the outcome of dividing ΔP by ΔV.

The variable step size used to perform tiny voltage adjustments is the fuzzy logic controller's output, and it is added to the solar voltage. This action also modifies the duty cycle of the photovoltaic voltage depending on the two inputs. When the delta power is equal to zero, the solar panel is said to be functioning at its maximum power point condition. When ΔP is greater than zero, the sign is positive, and vice versa. Similarly, when ΔV is positive, the voltage is updated by incorporating the minor adjustments obtained from the fuzzy logic controller's output. Employing MATLAB/Simulink, the fuzzy logic-based P&O for PV MPPT is established, simulated, and is discussed in the section that follows.

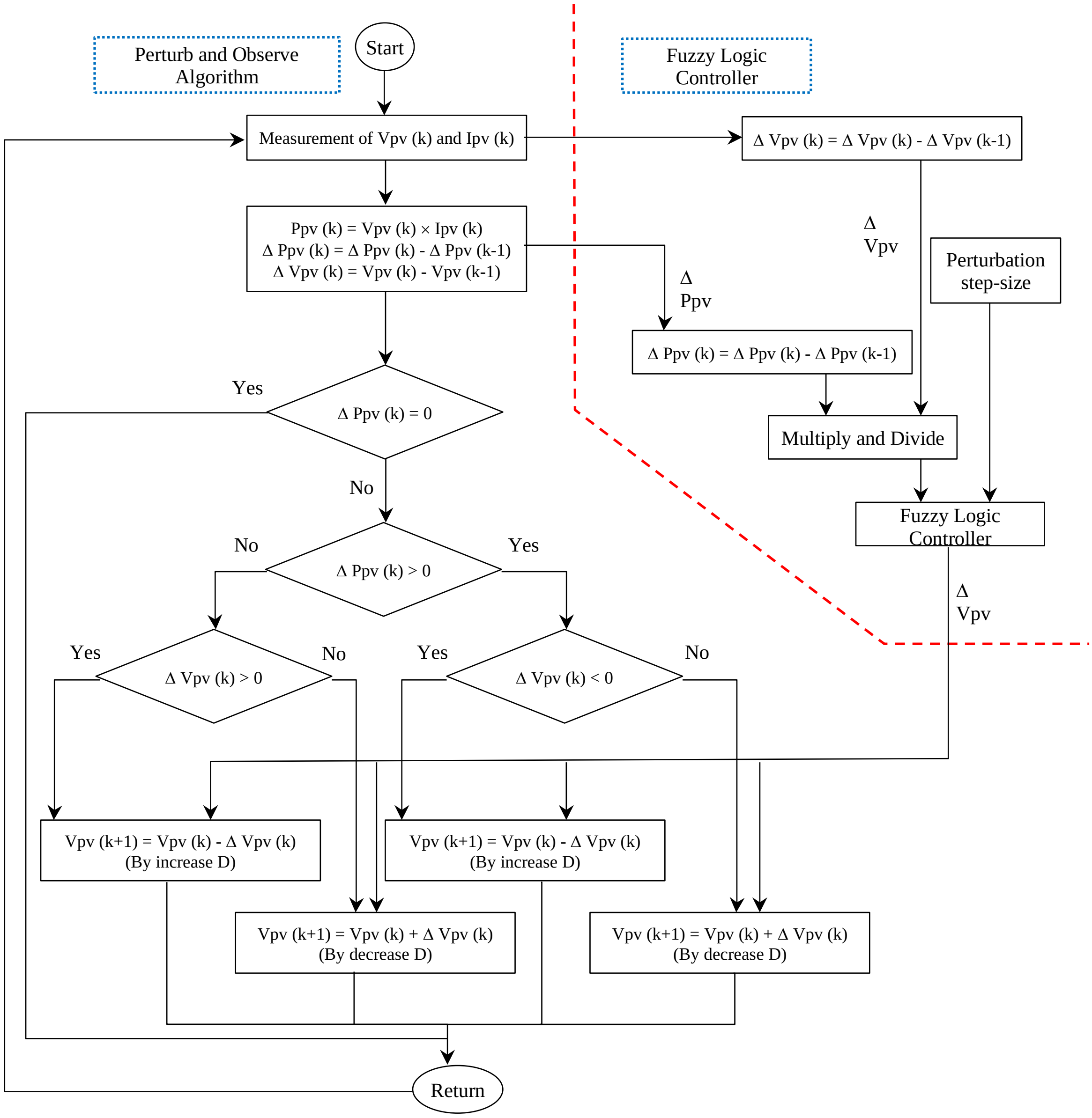


Figure 6. Fuzzy logic controller-based P&O flowchart for monitoring maximum power point

## 4. RESULTS AND DISCUSSION

### 4.1. Photovoltaic system circuit model

Next, as shown in Figure 7, the photovoltaic system circuit design is created employing MATLAB/Simulink software to assess system performance under various circumstances. This Simulink design includes loads, a boost converter, a solar module (1Soltech 1STH-250-WH), and an algorithm for MPPT that uses a fuzzy logic controller based on perturb and observe. The controller subsystem is depicted in Figure 8. The photovoltaic array with a capacity of 250.205 W consists of one series module and one parallel string. The loads considered in this model are 5, 30 and 100 Ω while the power converter used is IGBT with diode boost converter.

### 4.2. Fuzzy rule base

The fuzzy rule base is constructed using the fuzzy logic designer in MATLAB/Simulink. For the fuzzy inference system (FIS), the membership functions include two input variables and one output variable. The perturbation step size is expressed by the first input variable, FS, as shown in Figure 9. The second input, expressed as S in Figure 10, is ΔP/ΔV, or the P-V curve's slope. The fuzzy logic controller produces an output called the variable step size (VSS), as illustrated in Figure 11.

When the design of fuzzy logic finished, the rules and surface viewer presented in Figure 12 and Figure 13. There are 25 different rules corresponding between inputs and output of FIS variables. The example of if-then rule stated as:

$$1. If\ (A\ is\ X1)\ and\ (B\ is\ Y1)\ then\ (C\ is\ A1)$$
$$\dots\dots$$
$$25. If\ (A\ is\ X5)\ and\ (B\ is\ Y5)\ then\ (C\ is\ A25)$$

where $A$ = First input, $X1$ = First variable of first input, $B$ = Second input, $Y1$ = First variable of second input, $C$ = Output, $A1$ = First output and $A25$ = 25th output.

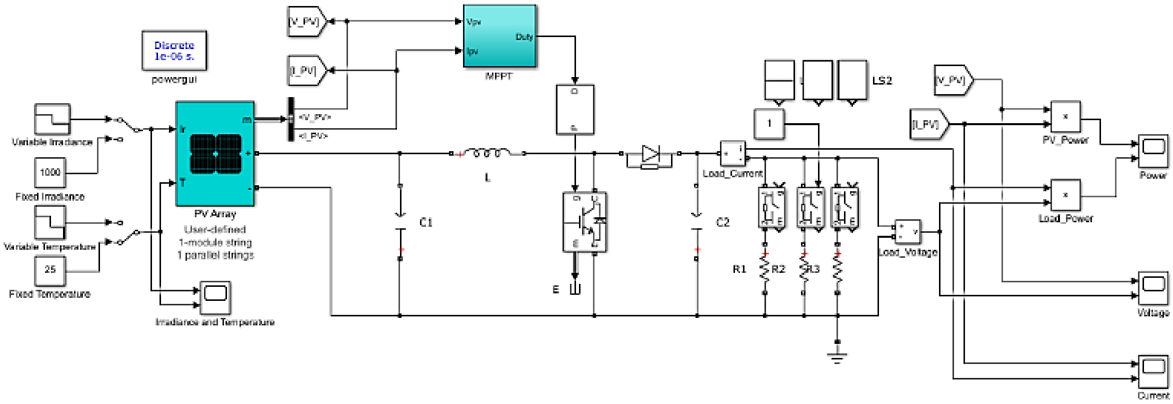


Figure 7. Simulation circuit

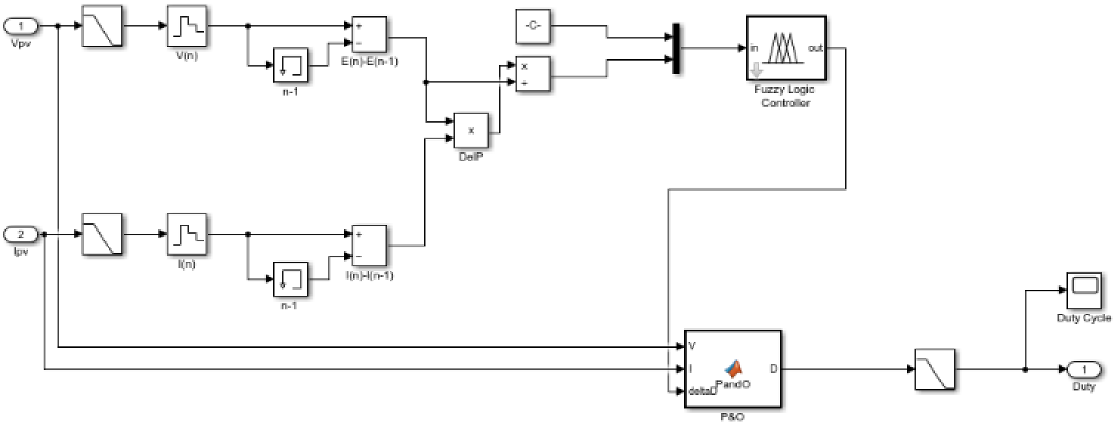


Figure 8. Maximum power point tracking controller subsystem

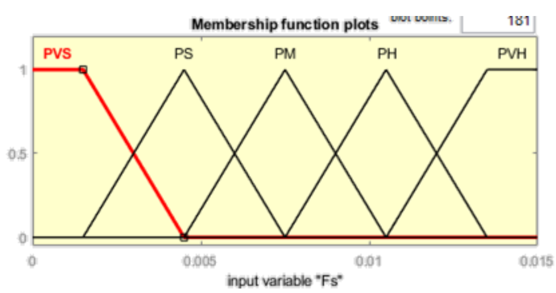


Figure 9. Input variable of perturbation step size, FS

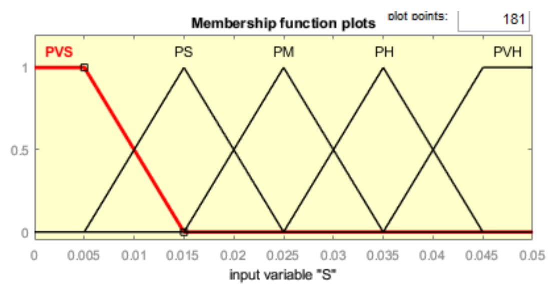


Figure 10. Input variable of P-V curve slope, S

The fuzzy rule consists of fixed variables A, B, and C, along with changing variables X1, Y1, and A1~A25, which represent the variable relationship according to the fixed variables. These rules are visualized in a 3-D dimension due to the presence of three different FIS variables, as shown in Figure 12. The complete set of rules are visible in the rule viewer depicted in Figure 13. The two inputs are altered as part of the fuzzy system's inference process in order to observe the matching output - that is, the defuzzified output values and the aggregated output fuzzy set, for every fuzzy rule. The P&O method completes when the fuzzy logic controller outputs the duty cycle (ΔD) change. Hence, this method is designed in the fuzzy logic-based perturb and observe approach to ensure that the PV output always remains in an optimal state.

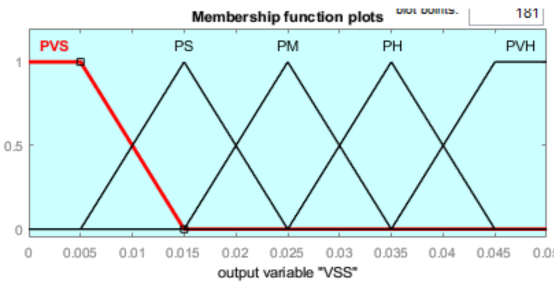


Figure 11. Variations in the variable step size, or VSS output

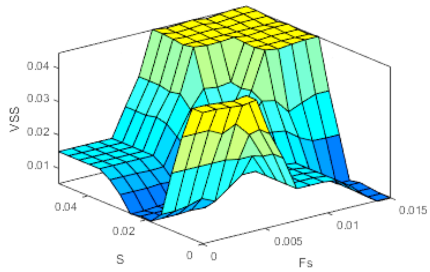


Figure 12. 3D Dimensions of fuzzy rule

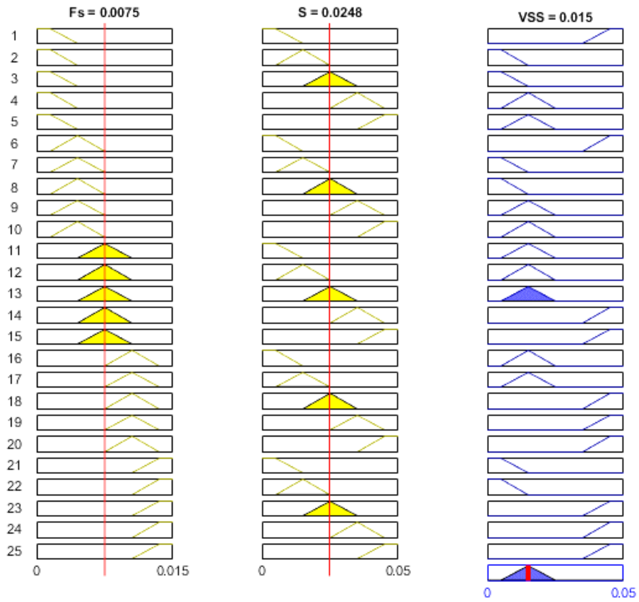


Figure 13. Rule viewer in MATLAB windows of fuzzy logic

### 4.3. Simulation result

#### 4.3.1. P-V and I-V curve

Based on Figures 14 and 15, the I-V curve characteristics represent the relationship between photovoltaic current (y-axis) and photovoltaic voltage (x-axis). Similarly, the P-V curve characteristics display the relationship between input photovoltaic power (y-axis) and photovoltaic voltage (x-axis). These graphs are plotted using the parameters of the 1Soltech 1STH-250-WH array and are displayed for two specific conditions: array @ 25 °C with specified irradiances and array @ 1,000 W/m² with specified temperatures. Various irradiance and temperature values are examined to track different states of the maximum power point. In Figure 14, the irradiance levels are varied from 1,000 W/m² to 400 W/m², while in Figure 15, the temperatures range from 85 °C to 25 °C. The red dot indicates the maximum power point and the corresponding maximum current at different voltages, as shown in Tables 3 to 6. These curves are correlated with the simulation results of the photovoltaic system circuit model. Furthermore, a comparison is made between the outputs of the boost converter with loads and the input of photovoltaic power.

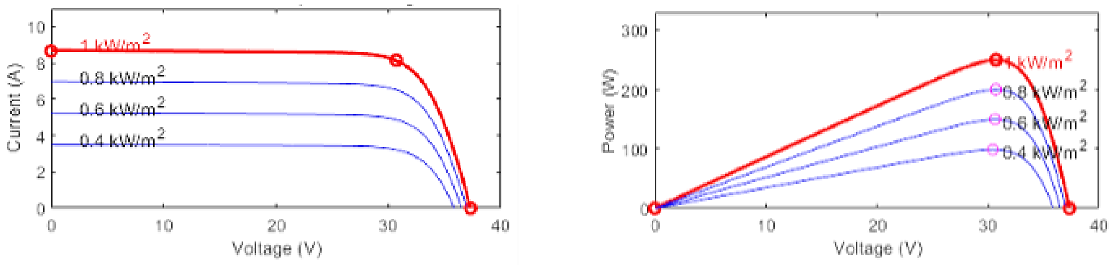


Figure 14. I-V and P-V curve characteristics for varying irradiance and fixed temperature

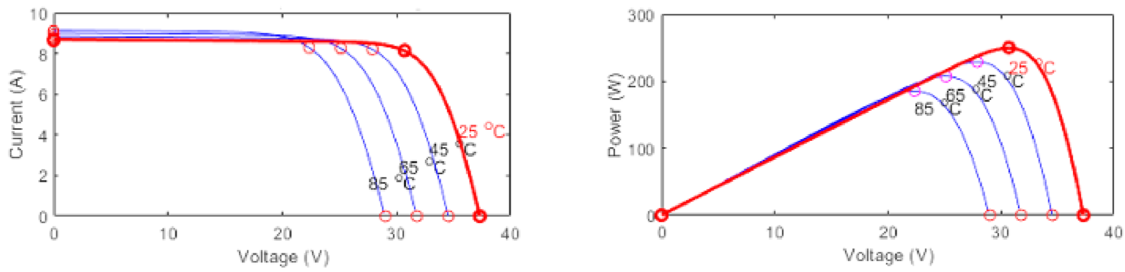


Figure 15. I-V and P-V curve characteristics for varying temperature and fixed irradiances

Table 3. Result of I-V curve characteristics for varying irradiance and fixed temperature

| Parameter | Variable irradiances (W/m²) & 25 °C temperature | | | |
|---|---|---|---|---|
| | 1,000 W/m² | 800 W/m² | 600 W/m² | 400 W/m² |
| | I-V curve characteristics | | | |
| Current (A) | 8.15 A | 6.52 A | 4.89 A | 3.26 A |
| Voltage (V) | 30.7 V | 30.68 V | 30.61 V | 30.41 V |

Table 4. Result of P-V curve characteristics for varying irradiance and fixed temperature

| Parameter | Variable irradiances (W/m²) & 25 °C temperature | | | |
|---|---|---|---|---|
| | 1,000 W/m² | 800 W/m² | 600 W/m² | 400 W/m² |
| | P-V curve characteristics | | | |
| Power (W) | 250.21 W | 200 W | 149.72 W | 99.03 W |
| Voltage (V) | 30.7 V | 30.68 V | 30.61 V | 30.41 V |

Table 5. Result of I-V curve characteristics for varying temperature and fixed irradiance

| Parameter | Variable temperature (°C) and 1,000 W/m² irradiance | | | |
|---|---|---|---|---|
| | 85 °C | 65 °C | 45 °C | 25 °C |
| | I-V curve characteristics | | | |
| Current (A) | 8.29 A | 8.26 A | 8.21 A | 8.15 A |
| Voltage (V) | 22.35 V | 25.12 V | 27.89 V | 30.7 V |

Table 6. Result of P-V curve characteristics for varying temperature and fixed irradiance

| Parameter | Variable temperature (°C) and 1,000 W/m² irradiance | | | |
|---|---|---|---|---|
| | 85 °C | 65 °C | 45 °C | 25 °C |
| | P-V curve characteristics | | | |
| Power (W) | 185.34 W | 207.4 W | 228.87 W | 250.21 W |
| Voltage (V) | 22.35 V | 25.12 V | 27.89 V | 30.7 V |

#### 4.3.2. Varying irradiance and fixed temperature

Figures 16 to 20 exhibit the findings of the simulation. This section focuses on the varying irradiance with a fixed temperature of 25 °C. The blue line in the graphs represents the photovoltaic array's initial condition, while the red line represents the output of the boost converter and loads. The simulation results are also tabulated in Table 7. Figure 17 shows a "ladder down-shape" profile, indicating that the power output varies with different irradiance levels. At $t$ = 0.1 s, when the irradiance is 1,000 W/m², the power at the maximum power point is approximately 250 W. Nevertheless, when the irradiance decreases to 800 W/m² at $t$ = 0.3 s, the power drops to around 200 W due to reduced irradiance reception. Both graphs demonstrate similar outputs in controlling the photovoltaic power to maintain stability and avoid voltage fluctuations. The explanation for these power outputs is provided in Figures 18 and 19. Figure 18 shows that at an irradiance of 1,000 W/m², the photovoltaic voltage is 31.54 V, while the load voltage is 60.95 V, as a result of the boost converter's nature to step up the system voltage. Similarly, Figure 19 illustrates that the photovoltaic current is 7.85 A, and the load current is 4.064 A, which is less than the input current due to the voltage increase in the boost converter at 1,000 W/m². This relationship aligns with Ohm's Law, where power is the product of voltage and current, as stated in the P&O subsystem. To achieve the maximum power point, the voltage or current needs to increase or decrease simultaneously. Hence, when the voltage reaches its maximum or rises, the current decreases. Lastly, Figure 20 shows the variation of the duty cycle, which follows the irradiance level. The initial duty cycle is 0.4808 and decreases proportionally with decreasing irradiance. Hence, the simulation results indicate that the proposed modified P&O based fuzzy logic controller exhibits excellent system performance by reducing steady-state oscillations close to the maximum power point and demonstrating a prompt reaction to irradiance fluctuations.

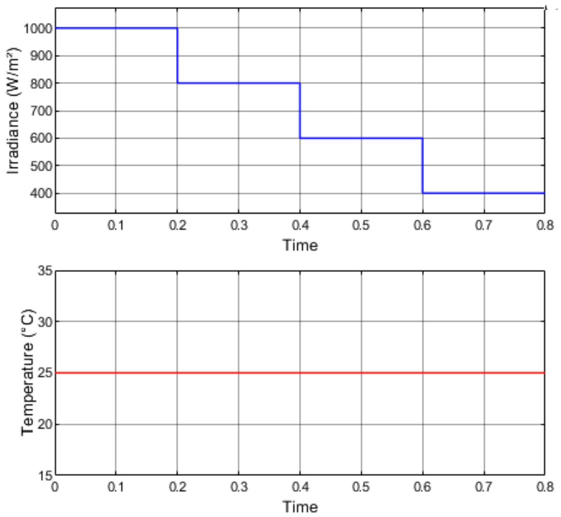


Figure 16. Varying irradiance and fixed temperature

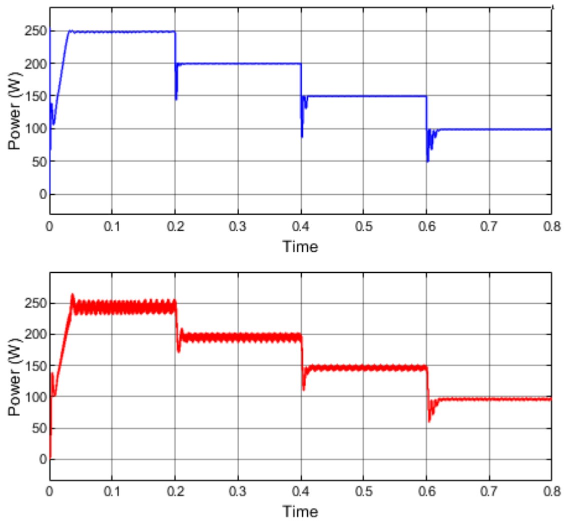


Figure 17. Photovoltaic power and load power

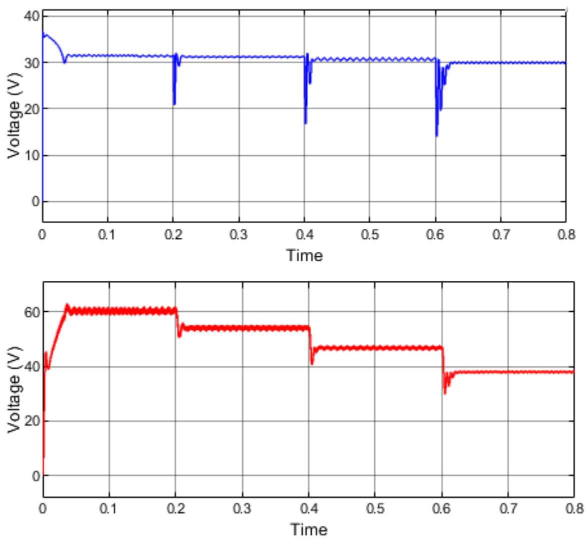


Figure 18. Photovoltaic voltage and load voltage

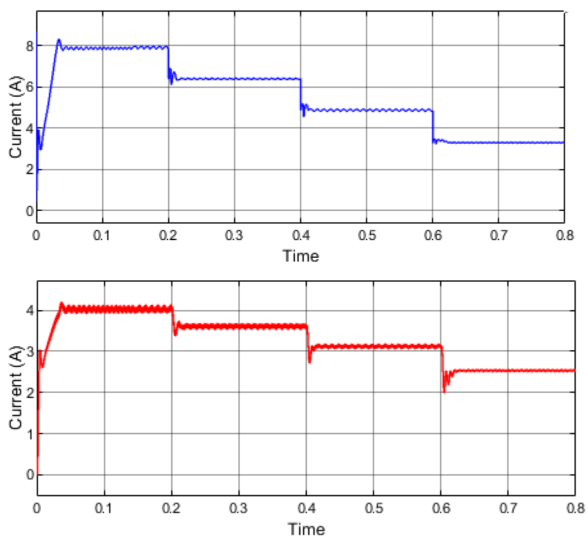


Figure 19. Photovoltaic current and load current

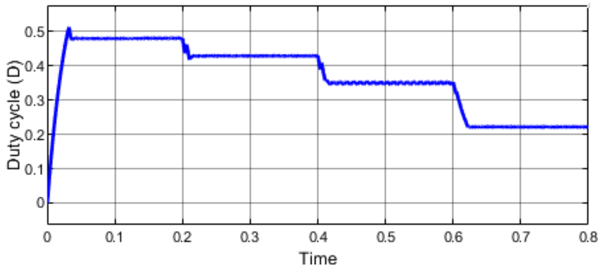


Figure 20. Duty cycle

Table 7. Result of varying irradiance and fixed temperature

| Parameter | Variable irradiances (W/m²) and 25°C temperature | | | | | | | |
|---|---|---|---|---|---|---|---|---|
| | 1,000 W/m² at 0.1 s | | 800 W/m² at 0.3 s | | 600 W/m² at 0.5 s | | 400 W/m² at 0.7 s | |
| | PV | Load | PV | Load | PV | Load | PV | Load |
| Power (W) | 247.6 W | 247.7 W | 199.4 W | 198.2 W | 149.5 W | 149.1 W | 98.89 W | 98.32 W |
| Voltage (V) | 31.54 V | 60.95 V | 31.22 V | 54.52 V | 30.98 V | 47.28 V | 29.99 V | 38.40 V |
| Current (A) | 7.85 A | 4.064 A | 6.388 A | 3.636 A | 4.827 A | 3.153 A | 3.298 A | 2.56 A |
| Duty cycle | 0.4808 | | 0.4305 | | 0.3502 | | 0.2198 | |

## 5. CONCLUSION

Photovoltaic panels are undeniably one of the most noticeable alternative techniques for generating renewable energy. However, a photovoltaic system without an MPPT algorithm faces challenges in harnessing the maximum power potential. An MPPT algorithm is needed to guarantee that the solar array runs at its peak efficiency. To gain advantages over the drawbacks of the ordinary fixed step size approach, an improved P&O MPPT algorithm with a fuzzy logic controller and variable step size was developed and put into practice. Simulation results indicate that the suggested approach responds to variations in irradiance more quickly and lessens steady-state oscillations near the maximum power point. The main objectives of this study were to evaluate and simulate the variable step size modifications of the P&O algorithm in a photovoltaic system using MATLAB/Simulink. Three criteria were analyzed, including power generated, current, voltage, and duty cycle, by comparing them with the P-V and I-V curve characteristics of the photovoltaic panel. Some of the disadvantages of employing a fixed step size in MPPT are addressed by the simulation findings, which show a trade-off between minimizing convergence time towards the maximum power point and eliminating oscillations in the solar array's power output around the maximum power point. Consequently, the primary goal of this paper, which aimed to examine the effectiveness of the improved P&O based fuzzy logic controller with a variable step size in a photovoltaic system, has been achieved.


## ACKNOWLEDGEMENTS

The authors would like to express their sincere gratitude for the generous funding, supervision, and resources provided by esteemed institutions, namely the Solar Research Institute (SRI) and the Research Management Centre (RMC) at Universiti Teknologi MARA (UiTM). Special thanks are extended to the College of Engineering at UiTM and the Faculty of Electrical Engineering at Universiti Teknikal Malaysia Melaka (UTeM) for their unwavering support and encouragement throughout this research undertaking. Additionally, the authors convey sincere appreciation to the Faculty of Sciences at Sidi Mohammed Ben Abdellah University, Morocco, for their invaluable contributions and collaborative efforts, significantly enhancing the scope and impact of this study. The successful accomplishment of this study would not have been achievable without the mentioned institutions, and for this, the authors are deeply appreciative.


## REFERENCES


[1] M. A. Abo-Sennah, M. A. El-Dabah, and A. E.-B. Mansour, “Maximum power point tracking techniques for photovoltaic systems: a comparative study,” *International Journal of Electrical and Computer Engineering (IJECE)*, vol. 11, no. 1, pp. 57–73, Feb. 2021, doi: 10.11591/ijece.v11i1.pp57-73.

[2] L. Abualigah *et al.*, “Wind, solar, and photovoltaic renewable energy systems with and without energy storage optimization: a survey of advanced machine learning and deep learning techniques,” *Energies*, vol. 15, no. 2, 2022, doi: 10.3390/en15020578.

[3] Vinod, R. Kumar, and S. K. Singh, “Solar photovoltaic modeling and simulation: as a renewable energy solution,” *Energy Reports*, vol. 4, pp. 701–712, Nov. 2018, doi: 10.1016/j.egyr.2018.09.008.

[4] S. S. Nadkarni, S. Angadi, and A. B. Raju, “Simulation and analysis of MPPT algorithms for solar PV based charging station,” in *2018 International Conference on Computational Techniques, Electronics and Mechanical Systems (CTEMS)*, Dec. 2018, pp. 45–50, doi: 10.1109/CTEMS.2018.8769191.

[5] B. E. Elnaghi, M. E. Dessouki, M. N. Abd-Alwahab, and E. E. Elkholy, “Development and implementation of two-stage boost converter for single-phase inverter without transformer for PV systems,” *International Journal of Electrical and Computer Engineering (IJECE)*, vol. 10, no. 1, pp. 660–669, Feb. 2020, doi: 10.11591/ijece.v10i1.pp660-669.

[6] A. Mohapatra, B. Nayak, and C. Saiprakash, “Adaptive perturb & observe MPPT for PV system with experimental validation,” in *2019 IEEE International Conference on Sustainable Energy Technologies (ICSET)*, Feb. 2019, pp. 257–261, doi: 10.1109/ICSETS.2019.8744819.

[7] K. Saidi, M. Maamoun, and M. Bounekhla, “Simulation and analysis of variable step size P&O MPPT algorithm for photovoltaic power control,” in *2017 International Conference on Green Energy Conversion Systems (GECS)*, Mar. 2017, pp. 1–4, doi: 10.1109/GECS.2017.8066265.

[8] A. I. M. Ali and H. R. A. Mohamed, “Improved P&O MPPT algorithm with efficient open-circuit voltage estimation for two-stage grid-integrated PV system under realistic solar radiation,” *International Journal of Electrical Power & Energy Systems*, vol. 137, May 2022, doi: 10.1016/j.ijepes.2021.107805.

[9] A. S. Samosir, H. Gusmedi, S. Purwiyanti, and E. Komalasari, “Modeling and simulation of fuzzy logic based maximum power point tracking (MPPT) for PV application,” *International Journal of Electrical and Computer Engineering (IJECE)*, vol. 8, no. 3, Jun. 2018, doi: 10.11591/ijece.v8i3.pp1315-1323.

[10] A. Al-Gizi, A. Hussien Miry, and M. A. Shehab, “Optimization of fuzzy photovoltaic maximum power point tracking controller using chimp algorithm,” *International Journal of Electrical and Computer Engineering (IJECE)*, vol. 12, no. 5, pp. 4549–4558, Oct. 2022, doi: 10.11591/ijece.v12i5.pp4549-4558.

[11] N. K. Pandey, R. K. Pachauri, S. Choudhury, and R. K. Sahu, “Asymmetrical interval Type-2 Fuzzy logic controller based MPPT for PV system under sudden irradiance changes,” *Materials Today: Proceedings*, vol. 80, pp. 710–716, 2023, doi: 10.1016/j.matpr.2022.11.074.

[12] R. Arulmurugan, “Optimization of perturb and observe based fuzzy logic MPPT controller for independent PV solar system,” *WSEAS Transactions on Systems*, vol. 19, pp. 159–167, Jul. 2020, doi: 10.37394/23202.2020.19.21.

[13] S. D. Al-Majidi, M. F. Abbod, and H. S. Al-Raweshidy, “A modified P&O-MPPT based on Pythagorean theorem and CV-MPPT for PV systems,” in *2018 53rd International Universities Power Engineering Conference (UPEC)*, Sep. 2018, pp. 1–6, doi: 10.1109/UPEC.2018.8542049.

[14] Z. M. S. Elbarbary and M. A. Alranini, “Review of maximum power point tracking algorithms of PV system,” *Frontiers in Engineering and Built Environment*, vol. 1, no. 1, pp. 68–80, Jul. 2021, doi: 10.1108/FEBE-03-2021-0019.

[15] R. Palanisamy, K. Vijayakumar, V. Venkatachalam, R. M. Narayanan, D. Saravanakumar, and K. Saravanan, “Simulation of various DC-DC converters for photovoltaic system,” *International Journal of Electrical and Computer Engineering (IJECE)*, vol. 9, no. 2, pp. 917–925, Apr. 2019, doi: 10.11591/ijece.v9i2.pp917-925.

[16] U. Yilmaz, A. Kircay, and S. Borekci, “PV system fuzzy logic MPPT method and PI control as a charge controller,” *Renewable and Sustainable Energy Reviews*, vol. 81, pp. 994–1001, Jan. 2018, doi: 10.1016/j.rser.2017.08.048.

[17] S. Singh, S. Manna, M. I. H. Mansoori, and A. K. Akella, “Implementation of perturb & observe MPPT technique using boost converter in PV system,” in *2020 International Conference on Computational Intelligence for Smart Power System and Sustainable Energy (CISPSSE)*, Jul. 2020, pp. 1–4, doi: 10.1109/CISPSSE49931.2020.9212203.

[18] M. Jiang, M. Ghahremani, S. Dadfar, H. Chi, Y. N. Abdallah, and N. Furukawa, “A novel combinatorial hybrid SFL–PS algorithm based neural network with perturb and observe for the MPPT controller of a hybrid PV-storage system,” *Control Engineering Practice*, vol. 114, Sep. 2021, doi: 10.1016/j.conengprac.2021.104880.

[19] N. Kumar, I. Hussain, B. Singh, and B. K. Panigrahi, “Framework of maximum power extraction from solar PV panel using self predictive perturb and observe algorithm,” *IEEE Transactions on Sustainable Energy*, vol. 9, no. 2, pp. 895–903, Apr. 2018, doi: 10.1109/TSTE.2017.2764266.

[20] M. N. Ali, K. Mahmoud, M. Lehtonen, and M. M. F. Darwish, “An efficient fuzzy-logic based variable-step incremental conductance MPPT method for grid-connected PV systems,” *IEEE Access*, vol. 9, pp. 26420–26430, 2021, doi: 10.1109/ACCESS.2021.3058052.

[21] T. Laagoubi, M. Bouzi, and M. Benchagra, “MPPT and power factor control for grid connected PV systems with fuzzy logic controller,” *International Journal of Power Electronics and Drive Systems (IJPEDS)*, vol. 9, no. 1, pp. 105–113, Mar. 2018, doi: 10.11591/ijpeds.v9.i1.pp105-113.

[22] X. Li, Q. Wang, H. Wen, and W. Xiao, “Comprehensive studies on operational principles for maximum power point tracking in photovoltaic systems,” *IEEE Access*, vol. 7, pp. 121407–121420, 2019, doi: 10.1109/ACCESS.2019.2937100.

[23] J. F. Silva and S. F. Pinto, “Linear and nonlinear control of switching power converters,” in *Power Electronics Handbook*, Elsevier, 2018, pp. 1141–1220.

[24] E. H. Mamdani and S. Assilian, “An experiment in linguistic synthesis with a fuzzy logic controller,” *International Journal of Man-Machine Studies*, vol. 7, no. 1, pp. 1–13, Jan. 1975, doi: 10.1016/S0020-7373(75)80002-2.

[25] M. Sugeno, *Industrial applications of fuzzy control*. Amsterdam, New York, N.Y., U.S.A: Elsevier Science Pub. Co, 1985.


## BIOGRAPHIES OF AUTHORS

**Muhammad Ihsan bin Aziz Jafar** is a graduate of the School of Electrical Engineering, College of Engineering, Universiti Teknologi MARA, Malaysia. He holds a bachelor's degree in electrical engineering from Universiti Teknologi Mara, which he obtained in 2023. His research interests revolve around sustainable energy, the impact of renewable energy sources on power quality, and photovoltaic systems. For further inquiries, he can be reached via email at ihsannashi99@gmail.com.

**Muhammad Iqbal Bin Zakaria** is a senior lecturer at School of Electrical Engineering, College of Engineering, Universiti Teknologi MARA (UiTM). He obtained his B.Eng degree in mechatronics from International Islamic University Malaysia in 2010 and his M.Eng and Ph.D degrees in electrical engineering from Universiti Teknologi Malaysia in 2012 and 2019 respectively. Starting his service in 2021, he brings a wealth of knowledge and expertise in the fields of renewable energy, photovoltaic systems, maximum power point tracking, fuzzy logic, stability of control systems via LMI approach and steer-by-wire of vehicle system. For inquiries, he can be contacted via email at iqbal.z@uitm.edu.my.

**Nofri Yenita Dahlan** earned her electrical engineering degree, B.Eng (Hons), from Universiti Tenaga Nasional (UNITEN), Malaysia in 2001. Subsequently, she pursued a master's degree (M.Sc.) at the University of Manchester Institute of Science and Technology (UMIST), UK, graduating in 2003. Later, she completed her Ph.D. in the field of energy economics at the University of Manchester, UK, in 2011. In recognition of her expertise, she was conferred with the Certified Measurement and Verification Professional (CMVP) credential by the Association of Energy Engineers (AEE) in 2013. Currently holding the position of Professor and Director at the Solar Research Institute (SRI), she can be reached via email at nofriyenita012@uitm.edu.my.

**Muhammad Nizam Kamarudin** received the M.Sc automation and control, Newcastle Upon Tyne, United Kingdom in 2006 until 2007, respectively, and the Ph.D. in electrical engineering, in University Teknologi Malaysia (UTM) in 2011 until 2015 and also B.Eng (Hons) in electrical engineering Universiti Teknologi Mara (UiTM). He has been a senior lecturer at University Teknologi Melaka (UTeM), since 2004. He is currently works at the Department of Control, Instrumentation and Automation, Universiti Teknikal Malaysia Melaka, Malacca, Malaysia. His research interests include Robust and Nonlinear Control Techniques, Stability of Uncertain System, Adaptive Backstepping and Fuzzy Control. He can be contacted at email: nizamkamarudin@utem.edu.my.

**Nabil El Fezazi** received his master's degree in engineering of automated industrial systems and his doctorate (PhD) in electrical engineering from the Sidi Mohammed Ben Abdellah University, Faculty of Sciences, Morocco in 2013 and 2018, respectively. His research and teaching interests focus on electrical, electronics, and computer engineering. He is the author of many articles and papers in refereed journals and international conferences in the areas of control systems (robust and $H_\infty$ control, observer-based control, sampled-data control, and fault tolerance control), fuzzy modeling, vehicle dynamics, TCP/IP networks, and wind tunnel. He can be contacted at email: nabil.elfezazi@gmail.com.